Received: 10 March 2020 | Revised: 17 June 2020 | Accepted: 22 June 2020

DOI: 10.1111/cas.14559

ORIGINAL ARTICLE

Cancer Science WILEY

lncRNA *IGKJ2-MALLP2* suppresses LSCC proliferation, migration, invasion, and angiogenesis by sponging *miR-1911-3p/p21*

Jing Cao[1,2] | Zhenming Yang[1] | Ran An[3] | Jiarui Zhang[1] | Rui Zhao[1] | Wenjing Li[1] | Licheng Xu[1,2] | Yanan Sun[1] | Ming Liu[1] | Linli Tian[1]

[1]Department of Otorhinolaryngology, Head and Neck Surgery, The Second Affiliated Hospital of Harbin Medical University, Harbin, China

[2]The Key Laboratory of Myocardial Ischemia, Ministry of Education, Harbin Medical University, Harbin, China

[3]Department of Otorhinolaryngology, Head and Neck Surgery, Heilongjiang Provincial Hospital Affiliated to Harbin Institute of Technology, Harbin, China

Correspondence
Ming Liu and Linli Tian, Department of Otorhinolaryngology, Head and Neck Surgery, The Second Affiliated Hospital of Harbin Medical University, Harbin, 150086, Heilongjiang Province, China.
Emails: liumingorg@163.com and tianlinli78@163.com

Funding information
National Natural Science Foundation of China, Grant/Award Number: 81572647; Natural Science Foundation of Heilongjiang Province, Grant/Award Number: LH 2019H014; Postgraduate Research & Practice Innovation Program of Harbin Medical University, Grant/Award Number: YJSKYCX2018-48HYD

Abstract

Because advanced laryngeal squamous cell carcinoma (LSCC) is diagnosed as a malignant tumor with a poor prognosis, the associated mechanisms still need to be further investigated. As key players in the development and progression of LSCC, lncRNAs have attracted increasing attention from many researchers. In this study, a novel lncRNA termed *IGKJ2-MALLP2* was identified and investigated for its effects on the development of LSCC. *IGKJ2-MALLP2* expression was confirmed by RT-qPCR in 78 pairs of tissues and human laryngeal carcinoma cell lines. The results of this study showed that the expression of *IGKJ2-MALLP2* was reduced in LSCC tissues and displayed close relationships with tumor stage, lymph node metastasis, and clinical stage. Using a dual-luciferase reporter assay, the ability of *miR-1911-3p* to bind both *IGKJ2-MALLP2* and *p21* mRNA was demonstrated. *IGKJ2-MALLP2* could upregulate *p21* expression by competitively binding *miR-1911-3p*. Moreover, *IGKJ2-MALLP2* effectively hindered the invasion, migration, and proliferation of AMC-HN-8 and TU212 tumor cells. Furthermore, its high expression could hinder the secretion of VEGF-A and suppress angiogenesis. As revealed by the results of in vitro experiments, *IGKJ2-MALLP2* overexpression could restrict tumor growth and blood vessel formation in a xenograft model of LSCC. As indicated from the mentioned findings, *IGKJ2-MALLP2*, which mediates *p21* expression by targeting *miR-1911-3p*, was capable of regulating LSCC progression and could act as an underlying therapeutic candidate to treat LSCC.

KEYWORDS
angiogenesis, lncRNA, LSCC, *p21*, progression

*These authors contributed equally to this work.

1 | INTRODUCTION

Laryngeal carcinoma is one of the most common tumors of the respiratory tract, and LSCC is the most common subtype.[1] In 2019 in the United States, 12 410 new cases of laryngeal carcinoma were reported and 3760 associated deaths with an incidence rate occurring for men and women of *c*. 4:1.[2] In particular, nearly 60% of patients are initially diagnosed at an advanced stage (stage III or IV),[3] resulting in laryngeal carcinoma as one of the few tumors with a decrease in the 5-y survival rate, from 66% to 63%, over the past 40 y.[4] Therefore, early diagnosis and therapy are required.

In many tumors, long noncoding RNAs (lncRNAs), which originate from the intergenic regions of mRNAs and are commonly transcribed by RNA polymerase II,[5,6] are longer than 200 nucleotides, and are considered to play crucial roles in tumor development and act as tumor suppressor or oncogenic genes to mediate the biological behaviors of tumor cells.[7,8] According to the results of some studies, lncRNA *MIR22HG* may participate in the progression of gastric cancer by mediating the Notch2 signaling pathways.[9] lncRNA *PCAT1* can facilitate tumor progression in many diseases.[10] Of note, some studies have also shown that lncRNAs are crucial to the development of LSCC.[11-14] These lncRNAs could compete for miRNA binding at shared response elements[15] or can bind to transcription factors to disrupt the targeted mRNA expression .[16] In our previous study, we identified a novel lncRNA, *IGKJ2-MALLP2* (ID: NONHSAT072221 in Noncode) from an RNA sequencing assay in which the expression of *IGKJ2-MALLP2* in tumor tissues was significantly lower than that observed in the adjacent tissues, and a follow-up analysis also showed that it might have an essential role in the development of laryngeal carcinoma.[17] In addition, Bu et al[18] also reported that the expression of *IGKJ2-MALLP2* was significantly altered in some tumors and adjacent tissues. Nevertheless, the role of *IGKJ2-MALLP2* in LSCC remains unclear. In the present study, we observed that in 78 patients with laryngeal carcinoma, *IGKJ2-MALLP2* expression in laryngeal carcinoma tissues was noticeably lower than that observed in adjacent tissues and was significantly associated with tumor stage, clinical stage and lymph node metastasis. Furthermore, *IGKJ2-MALLP2* could bind to *miR-1911-3p* and regulate the expression of *p21*, also known as cyclin-dependent kinase inhibitor 1A (CDKN1A), a well known protein associated with cancer. Low *p21* expression in laryngeal carcinoma can disrupt normal cell proliferation and differentiation and promote laryngeal carcinoma development.[19] Moreover, the results of in vitro experiments demonstrated that *IGKJ2-MALLP2* was involved in cell proliferation, metastasis, invasion, and angiogenesis-related activities. Therefore, the results of this study showed that *IGKJ2-MALLP2* may function as a powerful tumor biomarker for the diagnosis and treatment of laryngeal carcinoma.

2 | MATERIALS AND METHODS

2.1 | Clinical sample collection

From July 2016 to June 2018, 78 LSCC and matched adjacent noncancerous tissue (standard samples) specimens were harvested from patients at the Second Affiliated Hospital of Harbin Medical University and rapidly frozen in liquid nitrogen. All patients were first diagnosed with LSCC and then received total or partial laryngectomy with or without cervical lymph node dissection. No preoperative chemotherapy or neoadjuvant therapy was performed. All procedures complied strictly with the laryngeal carcinoma staging criteria of the American Joint Committee on Cancer (AJCC) staging system (8th version) in 2017. All informed consent forms were obtained from the patients, and the project was approved by the Ethics Committee of the Second Hospital of Harbin Medical University.

2.2 | Cell culture

Human bronchial epithelioid cells (16-HBE) and human laryngeal cancer cells (TU212 and AMC-HN-8) were obtained from the BeNa Culture Collection (BNCC), all of which were cultured routinely in high glucose Dulbecco's modified Eagle's medium (H-DMEM, HyClone) containing 10% fetal bovine serum (Biological Industries). Human umbilical vein endothelial cells (HUVECs) were purchased from the American Type Culture Collection (ATCC) and were cultured in endothelial cell medium (ECM; ScienCell). When the cells reached 90% confluency, they were passaged with a 0.25% trypsin-EDTA solution (Beyotime Biotechnology). The cells were cultured in a humidified incubator at 37°C under an atmosphere with 5% CO_2 in air (Thermo Fisher).

2.3 | Cell transfection

Using the lncRNA *IGKJ2-MALLP2* and *miR-1911-3p* sequences in the NCBI database (https://www.ncbi.nlm.nih.gov/gene/), lentiviruses expressing negative control (NC) RNA and lncRNA *IGKJ2-MALLP2* were developed by GeneChem Biotechnology in China, and a *miR-1911-3p* mimic and mimic-NC were designed by RiboBio in China. All of these sequences were transfected into cells in the logarithmic growth phase using Lipofectamine 2000 transfection reagent (Invitrogen) in accordance with the manufacturer's protocol. When transfection and verification were completed, the cells were used in subsequent experiments.

2.4 | Quantitative real-time PCR (RT-qPCR)

Cells used for RT-qPCR were cleaned with cold phosphate-buffered saline (PBS). Subsequently, total RNA was obtained using TRIzol Reagent (Invitrogen), and cDNA was generated from 2 μg of total RNA using a Transcriptor First Strand cDNA Synthesis kit (Roche Diagnostics). RNA expression was quantitatively assessed by RT-qPCR using a FastStart Universal SYBR Green Master kit (Roche Diagnostics). The relative expression levels of lncRNA *IGKJ2-MALLP2*, *p21* and *VEGF-A* were normalized to that of GAPDH, while those of *miR-1911-3p* were normalized to that of U6, with expression

levels calculated using the $2^{-\Delta\Delta CT}$ method. The sequences of primers used for RT-qPCR are presented in Table 1.

2.5 | Western blot (WB) analysis

For WB analysis, cells were lysed in RIPA buffer (Beyotime Biotechnology, China) supplemented with 1 mmol/L phenylmethanesulfonyl fluoride (Beyotime Biotechnology) and 1× protease inhibitor (Beyotime Biotechnology). The cell lysates were centrifuged, and the pelleted debris was discarded. Total protein was then mixed with 5× SDS-PAGE loading buffer and heated to 100°C for 5 min to prevent protein degradation. Protein samples (30 μg) were run on an SDS-PAGE gel and then transferred to a PVDF membrane. Subsequently, the membrane was blocked with 5% milk for 1 h and then incubated with the indicated primary antibody overnight. After being washed with TBS Tween (TBST) solution, the membrane was incubated with a secondary antibody and detected with enhanced chemiluminescence (ECL) reagents. Relative protein expression was analyzed using ImageJ software.

2.6 | Migration and invasion assay

Cells were seeded into the upper chamber of a 24-well transwell plate (Corning), while the lower chamber was filled with 0.6 mL of H-DMEM supplemented with 10% FBS. At the indicated times, the cells on the upper surface of the filter were scratched, while cells on the lower surface were fixed with 4% paraformaldehyde and stained with crystal violet. To identify the invasion ability of the cells, the upper chamber was coated with a layer of 20% Matrigel (Corning), and the subsequent procedures were performed as described above.

2.7 | Cell counting kit-8 (CCK-8) assay

To observe cell proliferation, a CCK-8 assay (Dojindo) was performed. Cells were seeded in 96-well plates (Corning) and, at the indicated times, 10 μL of CCK-8 solution was added to each well, after which the cells were incubated at 37°C for 2 h. The absorbance value of each well was measured at 450 nm and was reported as the cell viability.

2.8 | Colony formation assay

Cells were suspended in 2 mL of culture medium and then cultured in a 35-mm diameter Petri dish for 2 wk. The culture medium was replaced every other day and, after 2 wk, the cells were fixed with 4% paraformaldehyde and stained with crystal violet. Plates with positive colony formation were imaged.

2.9 | Cell-cycle analysis

Cells were seeded into 6-well plates and cultured overnight until reaching *c*. 60%-70% confluency. To perform cell-cycle analyses, cells were collected and resuspended in 500 μL of propidium iodide (PI)/RNase staining buffer for 30 min at 37°C in the dark. Subsequently, the cell cycle was analyzed by flow cytometry.

2.10 | Enzyme-linked immunosorbent assay (ELISA)

Transfected cells were cultured in complete medium until cells reached *c*. 90% confluency. Then, the culture supernatant was harvested and centrifuged to remove the cell debris, and the conditioned medium (CM) supernatant was aliquoted and stored at −80°C. Subsequently, the VEGF-A concentration in CM was measured using a commercial ELISA kit (R&D Systems).

2.11 | Angiogenesis assays

For tube formation assays, a 48-well plate was covered with Matrigel, and HUVECs were seeded and cultured in a mixed medium (CM/ECM, 50:50, v/v). At 6 h later, tube formation was observed under a microscope. For the aortic ring sprouting assay, thoracic aortas were acquired from a 6-wk-old Sprague-Dawley rat. Next, 2 ml-thick aortic rings were placed in a 48-well plate (Corning) and covered by Matrigel. Then, 50 μL of H-DMEM supplemented with 10% FBS and

TABLE 1 The sequences of specific primers

Primer	Forward primer (5' to 3')	Reverse primer (5' to 3')
IGKJ2-MALLP2 (for RT PCR)	GACATATCCTTCACGGTTCCC	GTGAGACATACATCACCCATCC
p21 (for qRT-PCR)	TCCAGCGACCTTCCTCATCCAC	TCCATAGCCTCTACTGCCACCATC
miR-1911-3p (for qPCR)	GCGCACCAGGCATTGTG	AGTGCAGGGTCCGAGGTATT
VEGF-A (for qPCR)	GTGACAAGCCAAGGCGGTGAG	GATGGTGGTGTGGTGGTGACATG
U6 (for qPCR)	CTCGCTTCGGCAGCACA	AACGCTTCACGAATTTGCGT
GAPDH (for qPCR)	ACCCACTCCTCCACCTTTGAC	TGTTGCTGTAGCCAAATTCGTT

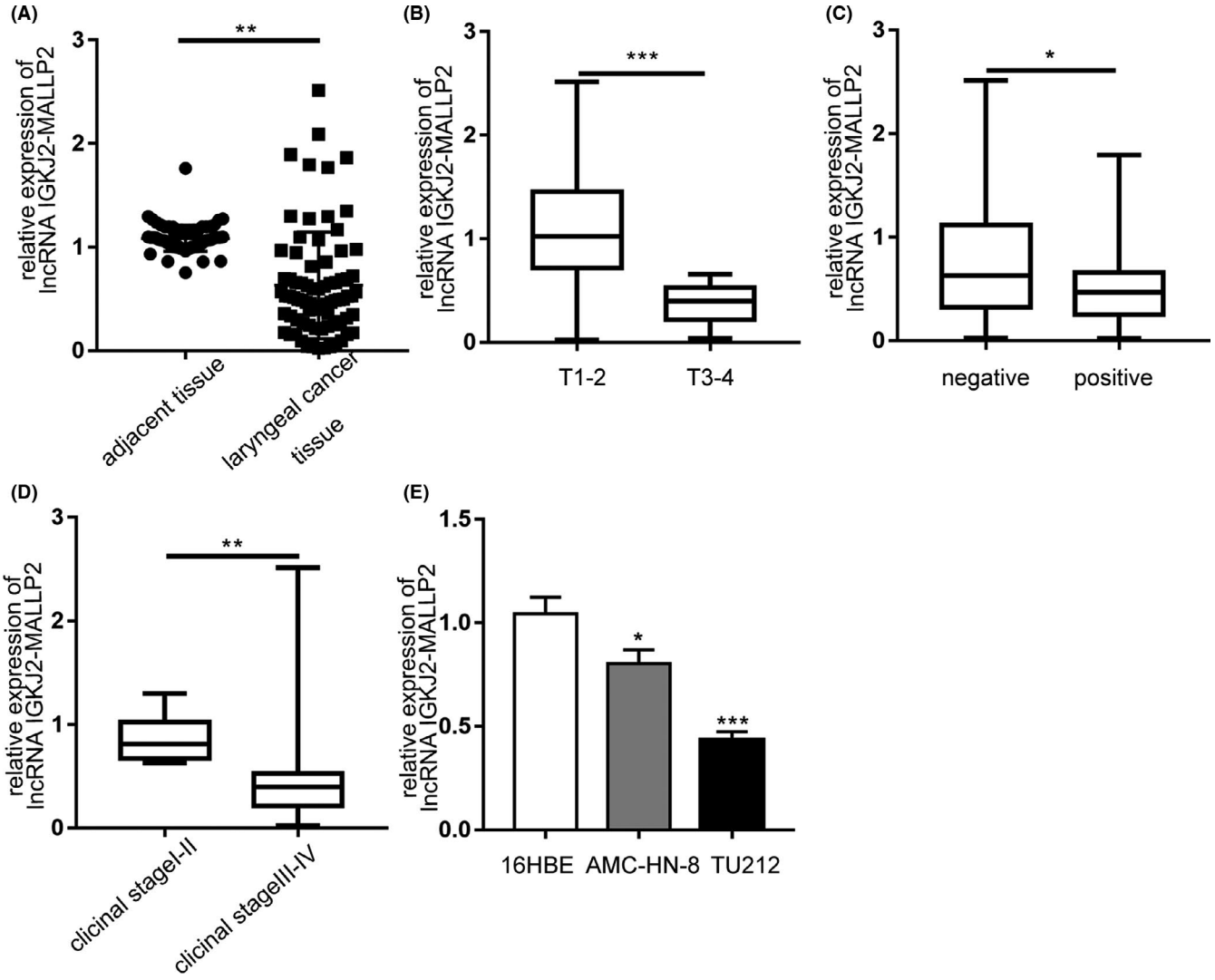

FIGURE 1 lncRNA *IGKJ2-MALLP2* expression in laryngeal carcinoma tissue and cell lines. A, The relative *IGKJ2-MALLP2* expression was ascertained by RT-qPCR in 78 pairs of laryngeal cancer and adjacent tissues. The relative expression in each group was normalized to that observed in the adjacent tissue. B-D, Relative *IGKJ2-MALLP2* expression in laryngeal cancer tissues with different tumor stages, lymph node metastasis, and clinical stages. E, Relative *IGKJ2-MALLP2* expression in laryngeal cancer cell lines. The data are presented as the means ± SD, $n = 3$; *, $P < .05$; **, $P < .01$; ***, $P < .001$

50 μL of CM was added to each well. Finally, 6 d later, the resulting mesh structures were imaged.

2.12 | Luciferase reporter assays

lncRNA-*IGKJ2-MALLP2*-WT, lncRNA-*IGKJ2-MALLP2*-MUT, *p21*-3'UTR-WT, and *p21*-3'UTR-MUT were obtained by PCR. After the correct sequences were confirmed by sequencing, *Not*I/*Xba*I-digested pcFLuc-Check2 fragments were ligated into a *Not*I/*Xba*I-digested plasmid. Luciferase assays were performed using 293T cells. Cells were seeded into 96-well plates, and, after reaching 50%-70% confluency, the cells were transfected with pSI-Check2-lnc*IGKJ2-MALLP2*-WT (or pSI-Check2-lnc*IGKJ2-MALLP2*-MUT) or pSI-Check2-*P21*-Wt (or pSI-Check2-*P21*-MUT) and the *miR-1911-3p* mimic or mimic-NC with Lipofectamine 3000 (Invitrogen). The luciferase activity in cell lysates was measured 48 h after cells were transfected with a Dual-Luciferase System (Luciferase Assay Reagent Promega).

2.13 | Animal xenograft tumor model

All animal experiments were approved by the Ethics Committee of Harbin Medical University, and the animal experiments were performed in the Second Affiliated Hospital of the Harbin Medical University. Here, 4-wk-old male nude BALB/c mice were provided by the Beijing Charles River Laboratory Animal Center and were fed and housed in pathogen-free cages. To observe tumor formation, TU212 cells stably expressing *IGKJ2-MALLP2* and NC under puromycin selection were identified. In total, 1×10^7 TU212 cells stably expressing of NC/*IGKJ2-MALLP2* were suspended in 200 μL of PBS

and injected hypodermically into the right side of BALB/c nude mice ($n = 6$). The mice were anesthetized with 3% isoflurane and euthanized by CO_2 inhalation. Subsequently, the tumors were removed, weighed, and fixed in 4% paraformaldehyde.

2.14 | Hematoxylin and eosin (H&E) staining

Tumor samples were embedded in paraffin and cut into 5 μm-thick sections before being dewaxed, hydrated, and stained with H&E.

2.15 | Immunohistochemistry (IHC)

The paraffin-embedded tumor tissues were removed from the paraffin and rehydrated for IHC, after which antigen recovery was performed under high pressure in an EDTA buffer solution. After incubation with primary and secondary antibodies, the slices were incubated with diaminobenzidine and counterstained with hematoxylin (Solarbio). Subsequently, the samples were imaged under a microscope (Olympus).

2.16 | Statistical analysis

All experiments were performed at least 3 times, and the data are presented as the mean values ± SEMs. One-way ANOVA and two-tailed Student *t* test were conducted to analyze differences between samples. The associations between *miR-1911-3p* and *IGKJ2-MALLP2* expression were determined by Spearman rank correlation. The correlations between *IGKJ2-MALLP2* expression and clinicopathological characteristics were assessed using a chi-squared (χ^2) test. Differences were considered significant at $P < .05$.

3 | RESULTS

3.1 | *IGKJ2-MALLP2* expression in laryngeal carcinoma tissue and laryngeal carcinoma cell lines

To assess the expression of *IGKJ2-MALLP2* in laryngeal carcinoma, 78 pairs of LSCC tissues and adjacent specimens were analyzed by RT-qPCR. The results showed that *IGKJ2-MALLP2* expression was considerably lower in laryngeal carcinoma tissues than that observed in adjacent normal tissues (Figure 1A). Specifically, *IGKJ2-MALLP2* expression was decreased in 84.6% (66/78) of the test samples. Moreover, the results suggested that the expression of *IGKJ2-MALLP2* was negatively associated with advanced clinical stage, lymph node metastasis and tumor stage in patients with laryngeal carcinoma (Figure 1B-D). To further evaluate the association between *IGKJ2-MALLP2* expression and clinical pathological characteristics, 78 human laryngeal carcinoma tissue samples were divided into 2 groups, the high *IGKJ2-MALLP2*-expressing group ($n = 39$) and the low *IGKJ2-MALLP2*-expressing group ($n = 39$), according to the median ratio of relative *IGKJ2-MALLP2* expression. The correlation analysis revealed that low *IGKJ2-MALLP2* expression was tightly associated with tumor stage ($P = .0225$), lymph node metastasis ($P = .0015$) and clinical stage ($P = .0012$). In contrast, drinking history, smoking history, age, and gender displayed no correlations with *IGKJ2-MALLP2* expression (Table 2). Furthermore, low *IGKJ2-MALLP2* expression was also observed in 16-HBE, AMC-HN8, and TU212 cells (Figure 1E).

TABLE 2 Correlations between *IGKJ2-MALLP2* and clinical characteristics of 78 laryngeal cancer patients

Characteristics	n	*IGKJ2-MALLP2* level		*P* value
		High	Low	
Total case	78	39	39	
Gender				
Male	65	30	35	.1287
Female	13	9	4	
Age (y)				
≤60	41	21	20	.9907
>60	37	19	18	
Smoking history				
Non-smokers	10	5	5	.8619
Current smokers	68	36	32	
Drinking				
Drinker	48	25	23	.6416
Non-drinker	30	14	18	
Tumor stage				
T1-T2	26	12	14	.0225*
T3-T4	52	11	41	
Lymph node				
Negative	30	19	11	.0015*
Positive	48	13	35	
Clinical stage				
I-II	21	13	8	.0012*
III-IV	57	13	44	

* $P < .05$.

3.2 | *IGKJ2-MALLP2* regulates cell proliferation, migration and invasion

After transfecting cells with the lentivirus, *IGKJ2-MALLP2* expression was increased in both *IGKJ2-MALLP2* groups of AMC-HN-8 and TU212 cells (Figure 2A). In the CCK-8 assay, the proliferation of cells was decreased after the overexpression of *IGKJ2-MALLP2* in both AMC-HN-8 and TU212 cells (Figure 2B). In the colony formation assay, the results showed that *IGKJ2-MALLP2* overexpression inhibited the formation of both AMC-HN-8 and TU212 tumor cell colonies (Figure 2C). To

elucidate the effects of *IGKJ2-MALLP2* on cell proliferation, cell-cycle assays were performed. The results showed that *IGKJ2-MALLP2* overexpression caused a notable increase in cell-cycle arrest at the G1-G0 phase in both AMC-HN-8 and TU212 cells (Figure 2D).

The migration and invasion abilities of tumor cells are crucial in tumor development. In the migration assay, the number of cells passing through the filter in the *IGKJ2-MALLP2* overexpression group was considerably decreased in both AMC-HN-8 and TU212 cells (Figure 2E). In the invasion assay, the number of AMC-HN-8 and TU212 cells that passed through the Matrigel was also reduced when they were transfected with the *IGKJ2-MALLP2* lentivirus (Figure 2F).

3.3 | *IGKJ2-MALLP2* suppresses VEGF-A expression and angiogenesis

Blood vessels are extremely important for tumor development. To elucidate the effects of *IGKJ2-MALLP2* on angiogenesis, tube

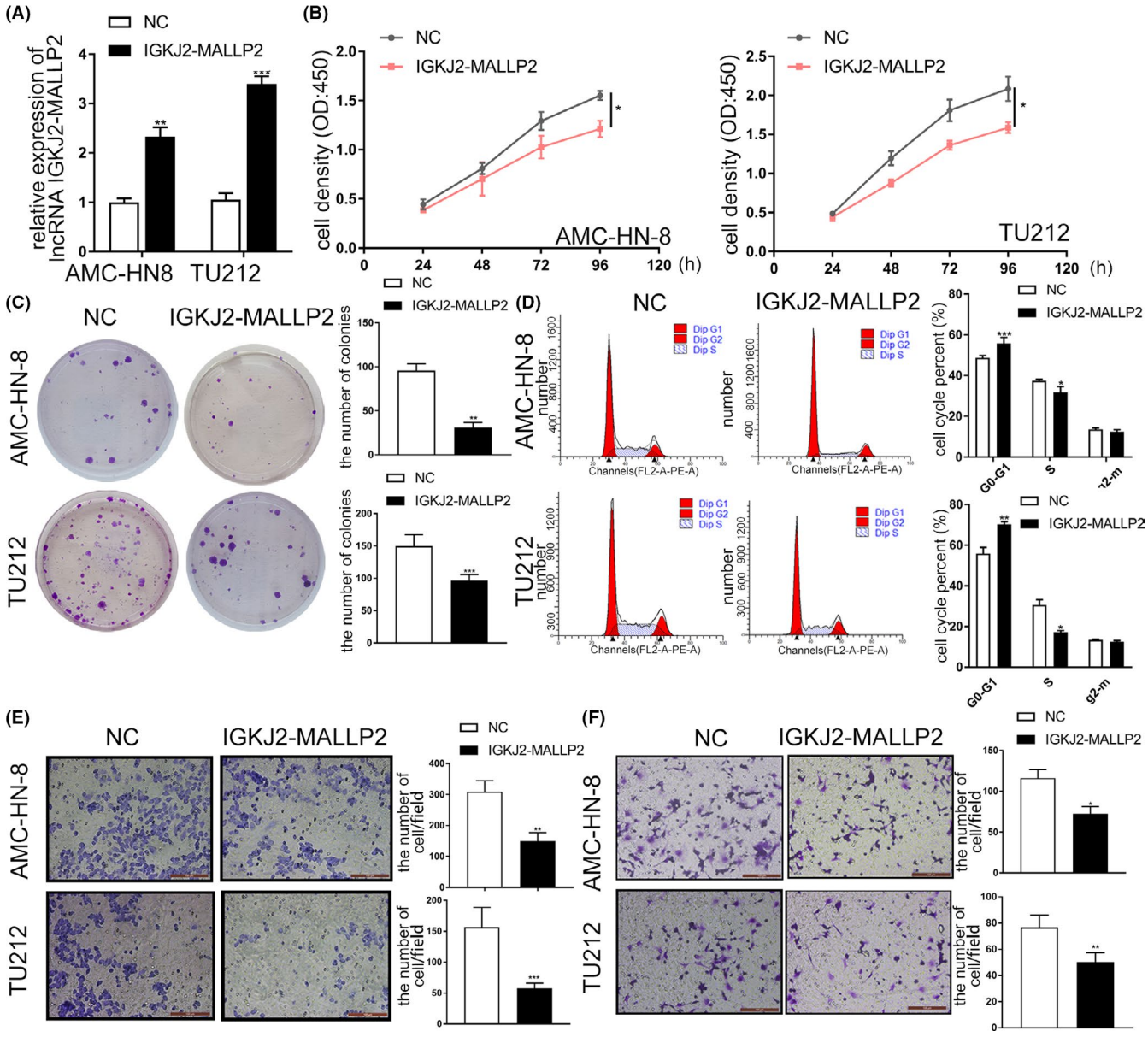

FIGURE 2 lncRNA *IGKJ2-MALLP2* regulates the proliferation, migration and invasion of TU212 cells. A, The relative expression of *IGKJ2-MALLP2* in AMC-HN-8 and TU212 cells after lentiviral transfection. B, CCK-8 assays to ascertain the proliferation of AMC-HN-8 and TU212 cells transfected with NC or *IGKJ2-MALLP2* lentivirus. C, Colony formation assays to assess the proliferation of AMC-HN-8 and TU212 cells transfected with NC or *IGKJ2-MALLP2* lentivirus. D, Effects of *IGKJ2-MALLP2* on the cell cycle of AMC-HN-8 and TU212 cells. E, The migration ability of AMC-HN-8 and TU212 cells transfected with NC or *IGKJ2-MALLP2* lentivirus. F, The invasion ability of AMC-HN-8 and TU212 cells transfected with NC or *IGKJ2-MALLP2* lentivirus. The data were presented as the means ± SD; $n = 3$; *, $P < .05$; **, $P < .01$; ***, $P < .001$

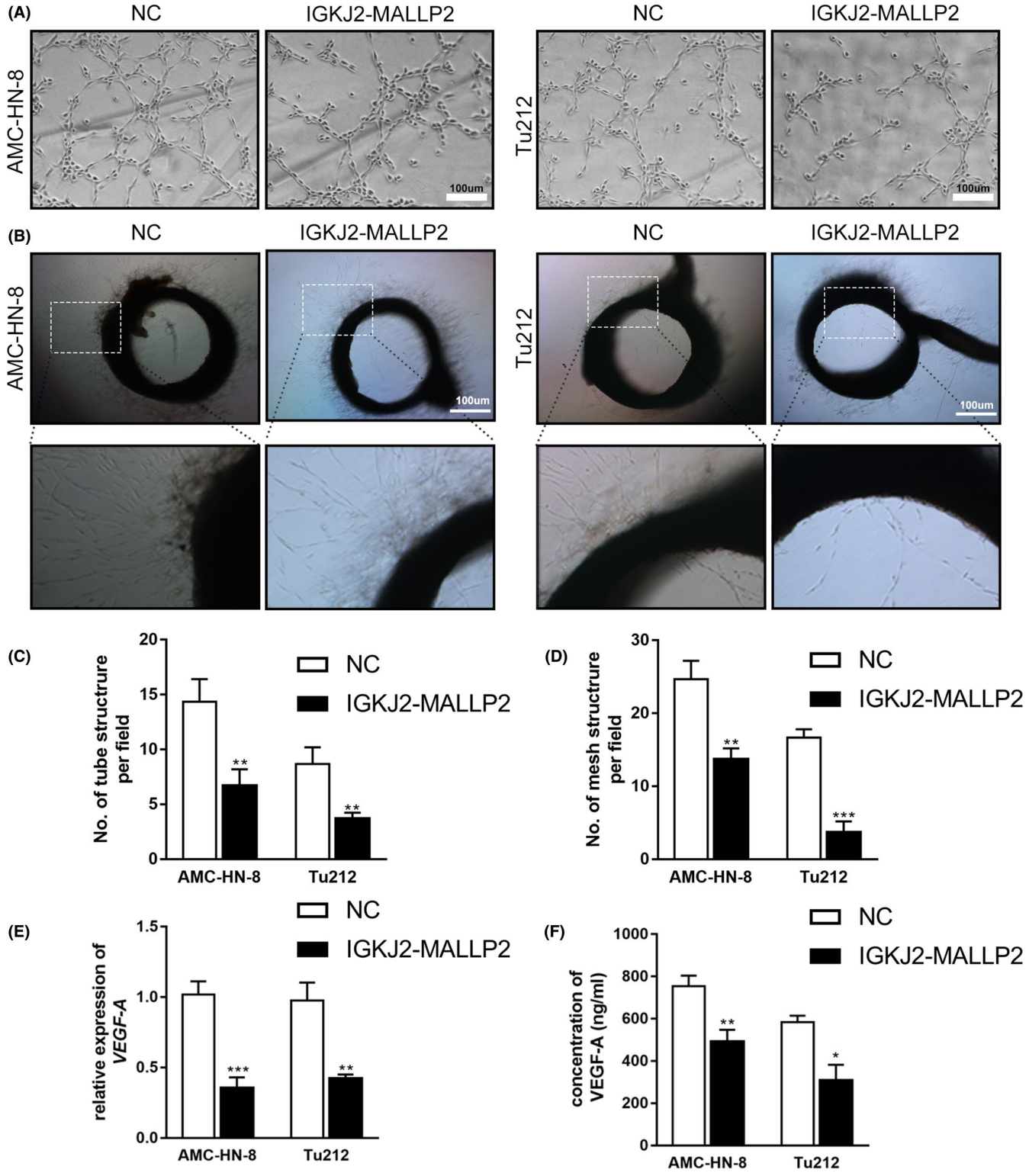

FIGURE 3 lncRNA *IGKJ2-MALLP2* suppresses angiogenic activities in vitro. A, The tube structures formed by HUVECs treated with CM from AMC-HN-8 and TU212 cell cultures. B, The mesh structures sprouting from aortic rings treated with CM from AMC-HN-8 and TU212 cell cultures. C, Quantitative analysis of tube structures. D, Quantitative analysis of mesh structures. E, Relative *VEGF-A* mRNA expression in AMC-HN-8 and TU212 cells transfected with NC or *IGKJ2-MALLP2* lentivirus. F, The concentration of VEGF-A in the culture supernatants of AMC-HN-8 and TU212 cells transfected with NC or *IGKJ2-MALLP2* lentivirus. The data are presented as the means ± SD, $n = 3$; *, $P < .05$; **, $P < .01$; ***, $P < .001$

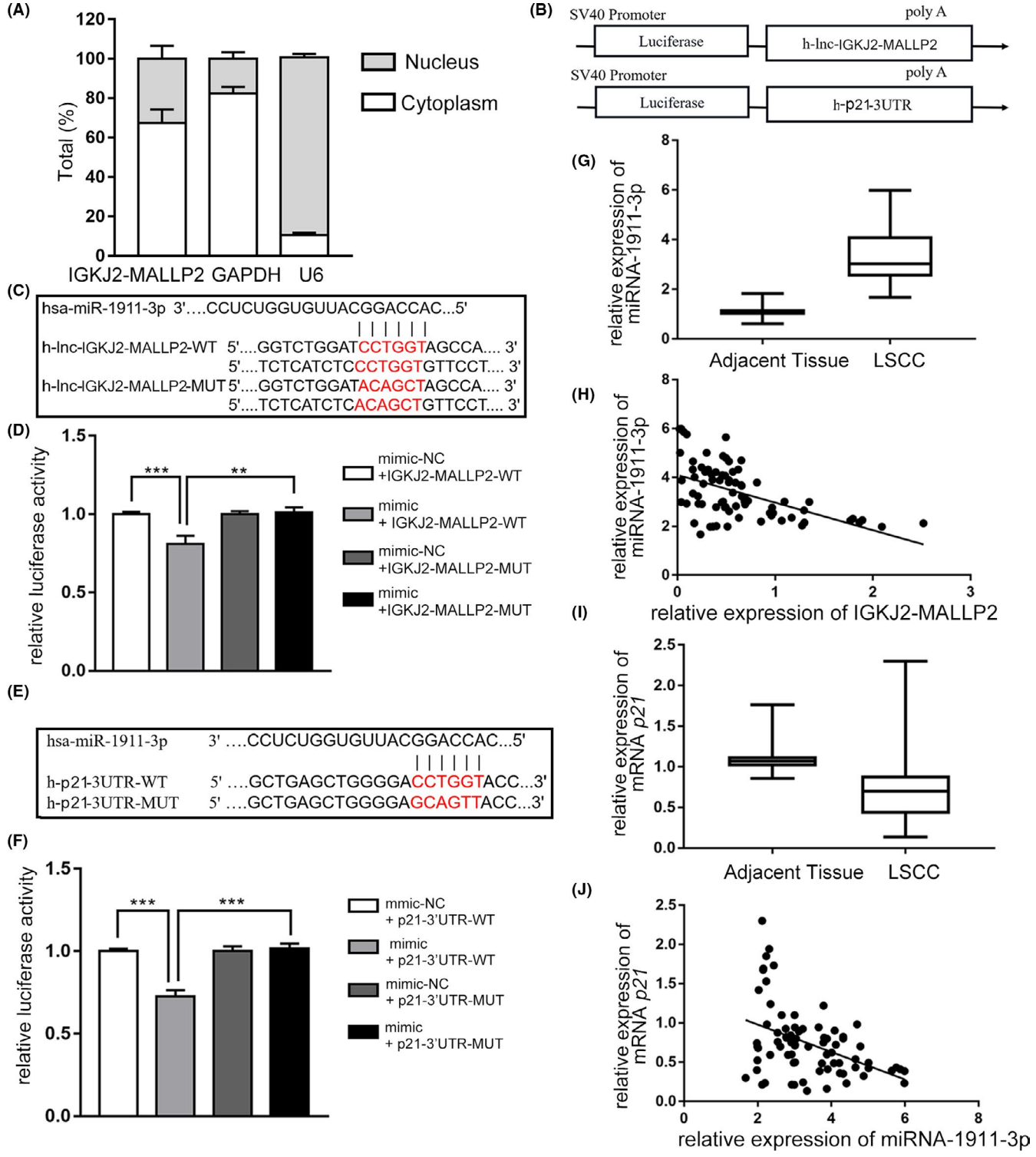

FIGURE 4 lncRNA *IGKJ2-MALLP2* binds *miR-1911-3p* to regulate *p21* in LSCC cells. A, The subcellular position of *IGKJ2-MALLP2* was ascertained in the cytoplasm or nucleus using GAPDH and U6 as cytoplasmic and nuclear controls, respectively ($P < .05$). B, Illustration showing the vector structure of *IGKJ2-MALLP2* and *p21*-3'UTR. C, The potential binding sites of *miR-1911-3p* and *IGKJ2-MALLP2*. D, Luciferase reporter assay results demonstrated the interaction between *miR-1911-3p* and *IGKJ2-MALLP2*. E, The potential binding sites of *miR-1911-3p* and *p21*-3'UTR. F, Luciferase reporter assay results demonstrated the interaction between *miR-1911-3p* and *p21*-3'UTR. G, The level of *miR-1911-3p* expression in laryngeal cancer and noncancerous tissues ($n = 78$). H, Spearman's correlation analysis between *miR-1911-3p* and *IGKJ2-MALLP2* levels in LSCC tissues ($n = 78$, $P < .001$). I, The level of mRNA *p21* expression in laryngeal cancer and noncancerous tissues ($n = 78$). J, Spearman's correlation analysis between *miR-1911-3p* and *p21* levels in LSCC tissues ($n = 78$, $P < .01$). The data are presented as the means ± SD, $n = 3$ **; $P < .01$; ***, $P < .001$

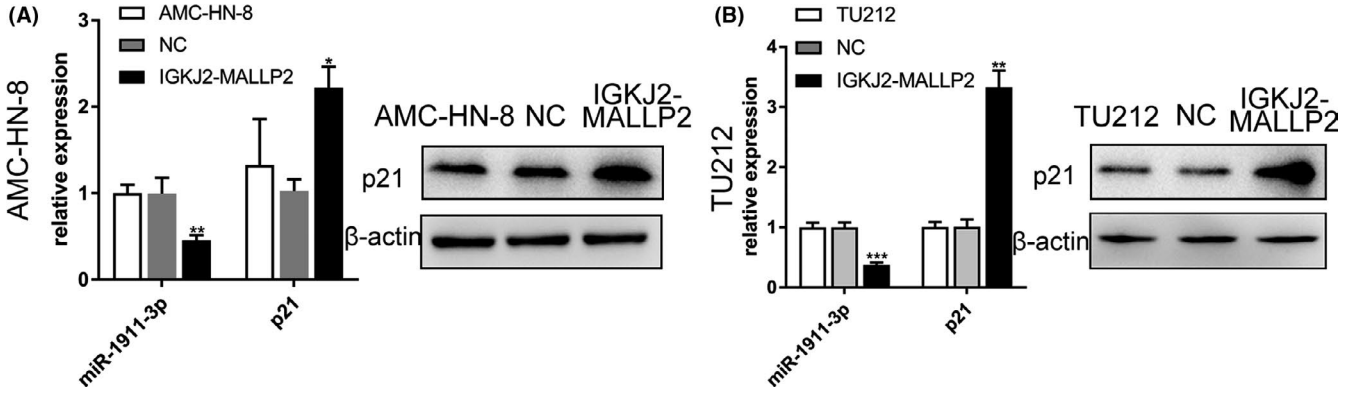

FIGURE 5 Verification of *miR-1911-3p* and *p21* expression in cells overexpressing *IGKJ2-MALLP2*. A, The expression of *miR-1911-3p* and *p21* in AMC-HN-8 cells transfected with or without NC or *IGKJ2-MALLP2* lentivirus. B, The expression of *miR-1911-3p* and *p21* in TU212 cells transfected with or without NC or *IGKJ2-MALLP2* lentivirus. The data are presented as the means ± SD, $n = 3$; *, $P < .05$; **, $P < .01$; ***, $P < .001$

formation and aortic ring sprouting assays were performed. In contrast with that observed using CM from the NC group, the number of tube structures formed by HUVECs decreased when they were incubated in CM from both the AMC-HN-8 and TU212 *IGKJ2-MALLP2*-overexpressing groups (Figure 3A, C). In the aortic ring sprouting assay, fewer mesh structures were also observed in CM from the *IGKJ2-MALLP2* overexpression group than that observed in CM from NC group for both AMC-HN-8 and TU212 cells (Figure 3B, D). Due to its role as one of the most important cytokines to promote angiogenesis, we measured the levels of VEGF-A in CM from AMC-HN-8 and TU212 cells. The RT-qPCR results showed that *IGKJ2-MALLP2* overexpression inhibited the mRNA expression of *VEGF-A* in both AMC-HN-8 and TU212 cells (Figure 3E). In addition, the concentration of VEGF-A in the culture supernatant was also decreased when AMC-HN-8 and TU212 cells were transfected with the *IGKJ2-MALLP2* lentivirus (Figure 3F).

3.4 | *IGKJ2-MALLP2* regulates LSCC cells by sponging *miR-1911-3p/p21*

To elucidate how lncRNA *IGKJ2-MALLP2* functions, in this study, the *IGKJ2-MALLP2* contents in nuclear and cytoplasmic cell fractions were determined separately. The results showed that *IGKJ2-MALLP2* primarily occurs in the cytoplasm (Figure 4A). As it has been reported that lncRNA in cytoplasm could realize its function by ceRNA,[20] we wanted to assess the sponging activity of *IGKJ2-MALLP2*. After creating the vector structure of *IGKJ2-MALLP2* and *p21*-3'UTR (Figure 4B), *miR-1911-3p* was predicted to interact with lncRNA *IGKJ2-MALLP2* and *p21* using DIANA-LncBase v.2.0, TargetScan 7.2 and MiRTarBase 7.0 software. We identified the corresponding targets for lncRNA *IGKJ2-MALLP2*, *miR-1911-3p* and *p21*-3'UTR (Figure 4C, E), after which the associated mechanism was verified in cells using dual-luciferase reporter assays. The present study showed that in contrast with cells cotransfected with mimic-NC and *IGKJ2-MALLP2*-WT, the luciferase activity of cells cotransfected with the *miR-1911-3p* mimic and *IGKJ2-MALLP2*-WT was considerably decreased, whereas no change in activity was observed in cells cotransfected with the mimic and *IGKJ2-MALLP2*-MUT (Figure 4D). Similarly, in contrast with that observed in cells cotransfected with mimic-NC and *p21*-WT, the luciferase activity of cells cotransfected with the mimic and *p21*-WT was considerably decreased, whereas no change in activity was observed in cells cotransfected with the mimic and *p21*-MUT (Figure 4F). The expression of *miR-1911-3p* and *p21* mRNA in LSCC tissue was assessed, and the results revealed that *miR-1911-3p* exhibited high expression (Figure 4G) that was inversely correlated with *IGKJ2-MALLP2* expression (Figure 4H), whereas *p21* exhibited low expression (Figure 4I) that was inversely correlated with *miR-1911-3p* expression (Figure 4J).

To further investigate the *IGKJ2-MALLP2/miR-1911-3p/p21* axis, AMC-HN-8 and TU212 cells were transfected with the NC or *IGKJ2-MALLP2* lentivirus. Compared with that observed in cells transfected with the NC lentivirus, the expression of *miR-1911-3p* was decreased and the mRNA/protein expression of *p21* was increased in cells transfected with the *IGKJ2-MALLP2* lentivirus (Figure 5A, B).

3.5 | *IGKJ2-MALLP2* binds *miR-1911-3p* to regulated *p21* in TU212 cells

TU212 cells were transfected with the *miR-1911-3p* mimic or mimic-NC and the *IGKJ2-MALLP2* or NC lentivirus. In contrast with that observed in the NC + mimic-NC group, the expression of *miR-1911-3p* was increased in the NC + mimic group (Figure 6A). The expression of *miR-1911-3p* was lower in the *IGKJ2-MALLP2* + mimic group than that observed in the NC + mimic group (Figure 6A). To further demonstrate the relationships between *IGKJ2-MALLP2* and *miR-1911-3p/p21*, the expression of *p21* in each group was assessed. The results showed that the *p21* mRNA and protein levels in the NC + mimic group were the lowest among the 3 groups (Figure 6A, B). The CCK-8 assay results confirmed that cell proliferation in the

NC + mimic group was greater than that observed in the NC + mimic-NC and *IGKJ2-MALLP2* + mimic groups (Figure 6C). In contrast with that observed in the NC + mimic-NC and *IGKJ2-MALLP2* + mimic groups, the number of tumor colonies in the NC + mimic group was increased (Figure 6D, G). Furthermore, the migration and invasion abilities of TU212 cells in the NC + mimic group was also increased compared to that observed in the NC + mimic-NC and *IGKJ2-MALLP2* + mimic groups (Figure 6E, F, H, I).

3.6 | Effect of *IGKJ2-MALLP2* in vivo

The tumor formation of TU212 cells overexpressing *IGKJ2-MALLP2* in mice was smaller and lighter than that of TU212 cells transfected with the NC lentivirus in vivo (Figure 7A-C). The IHC staining results showed increased *p21* expression in the *IGKJ2-MALLP2* overexpression group (Figure 7D, E), while H&E staining results showed the presence of fewer blood vessels in the *IGKJ2-MALLP2* overexpression group (Figure 7F, G).

4 | DISCUSSION

As one of the most common head and neck squamous cell carcinomas, LSCC causes substantial economic and health burdens to society worldwide.[1] Because the incidence of LSCC grows every year,[13] it is urgent to understand the pathogenesis of LSCC and discover new diagnostic biomarkers for better treatments. The results of the

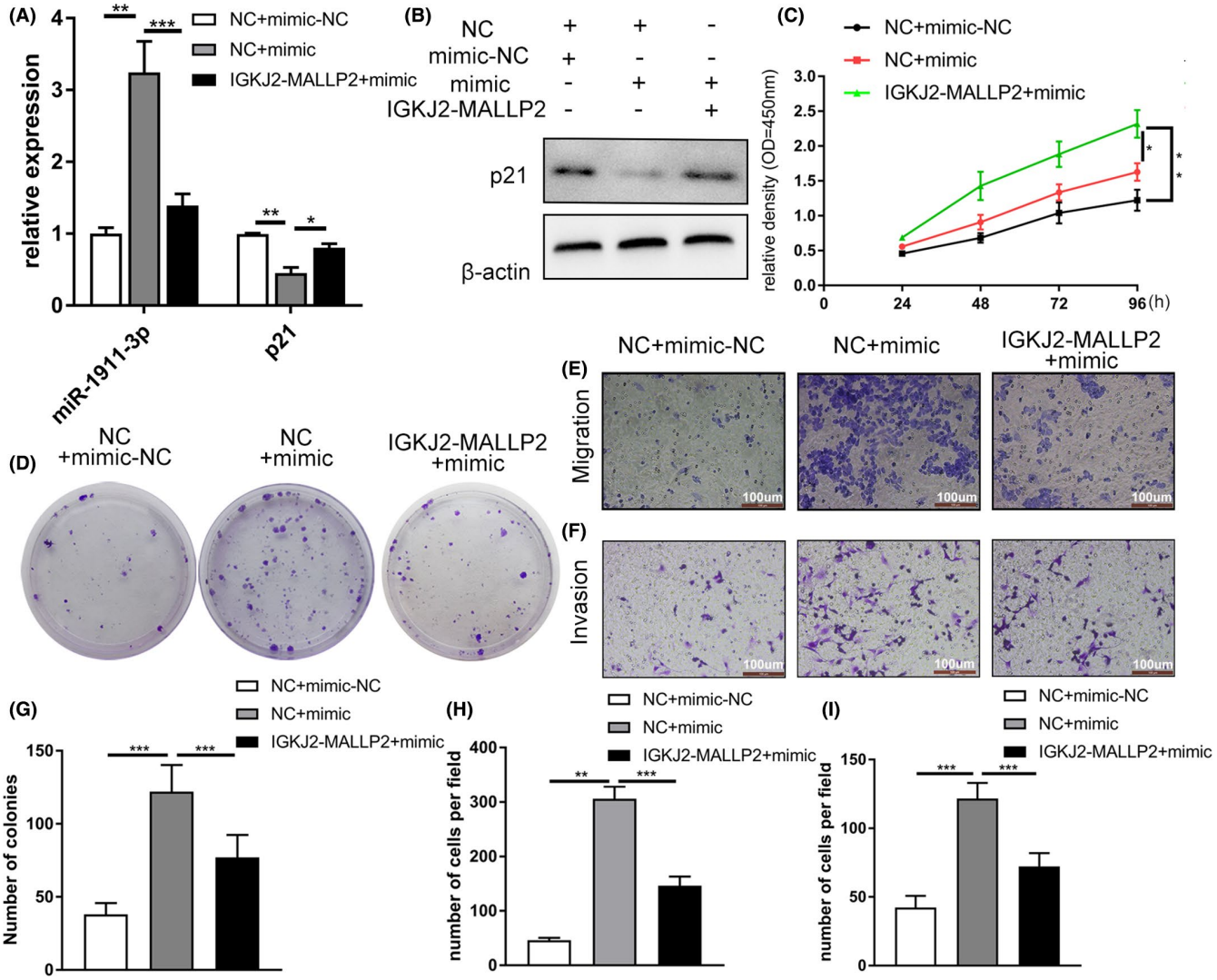

FIGURE 6 Verification of the relationships between *IGKJ2-MALLP2* and *miR-1911-3p/p21* in TU212 cells. A, The relative expression of *miR-1911-3p* and *p21* mRNA in TU212 cells with different transfections. B, The protein levels of *p21* in each group were ascertained by WB and normalized to β-actin. C, The proliferation of TU212 cells in different groups was examined by CCK-8 assay. D, Colony formation assays to ascertain the proliferation ability of TU212 cells. E, Migration assays to ascertain the cell migration ability of TU212 cells with different treatments. F, Invasion assays to analyze the invasive ability of cells. G, Quantitative analysis of colonies in the different groups. H, Quantitative analysis of the number of TU212 cells migrating through the filter. I, Quantitative analysis of the number of TU212 cells passing through the filter and Matrigel. The data are presented as the means ± SD; $n = 3$; *, $P < .05$; **, $P < .01$; ***, $P < .001$

present study demonstrated that *IGKJ2-MALLP2* had a clear regulatory role in LSCC in vitro and in vivo and may be a new therapeutic target.

lncRNAs are the largest and most diverse category of noncoding transcripts, and up to 60 000 lncRNA genes are present in the human genome.[6] These genes can interact with protein molecules, RNA or DNA, regulating gene expressions and affecting cellular processes through different mechanisms.[21] Although a considerable number of lncRNAs have been identified in the human genome, only a few genes have been experimentally verified and annotated in carcinomas. For instance, in non-small-cell lung cancer, lncRNA *NEAT1* has been shown to regulate tumor progression and apoptosis and to induce CSC-like phenotypic variations by interacting with RNA or protein.[22-24] lncRNA *NEAT1* has been also shown to be highly expressed in nasopharyngeal cancer and LSCC and can regulate radio-resistance, proliferation, invasion and apoptosis.[25,26] In addition, some other important lncRNAs (eg, *H19*,[27] *NOTCH1*,[28] *MALAT1*[29] and *HOTAIR*[30]) were proven to be expressed in both tumors and adjacent tissues. Furthermore, some lncRNAs expressed in laryngeal carcinomas have been studied. For instance, lncRNA *FOXD2-AS1* was shown to enhance chemotherapy resistance in LSCC by activating STAT3.[31] And, in the present study, the novel lncRNA *IGKJ2-MALLP2* was shown to have low expression in laryngeal carcinoma tissues and high expression in the normal adjacent tissues. When *IGKJ2-MALLP2* expression was increased in laryngeal

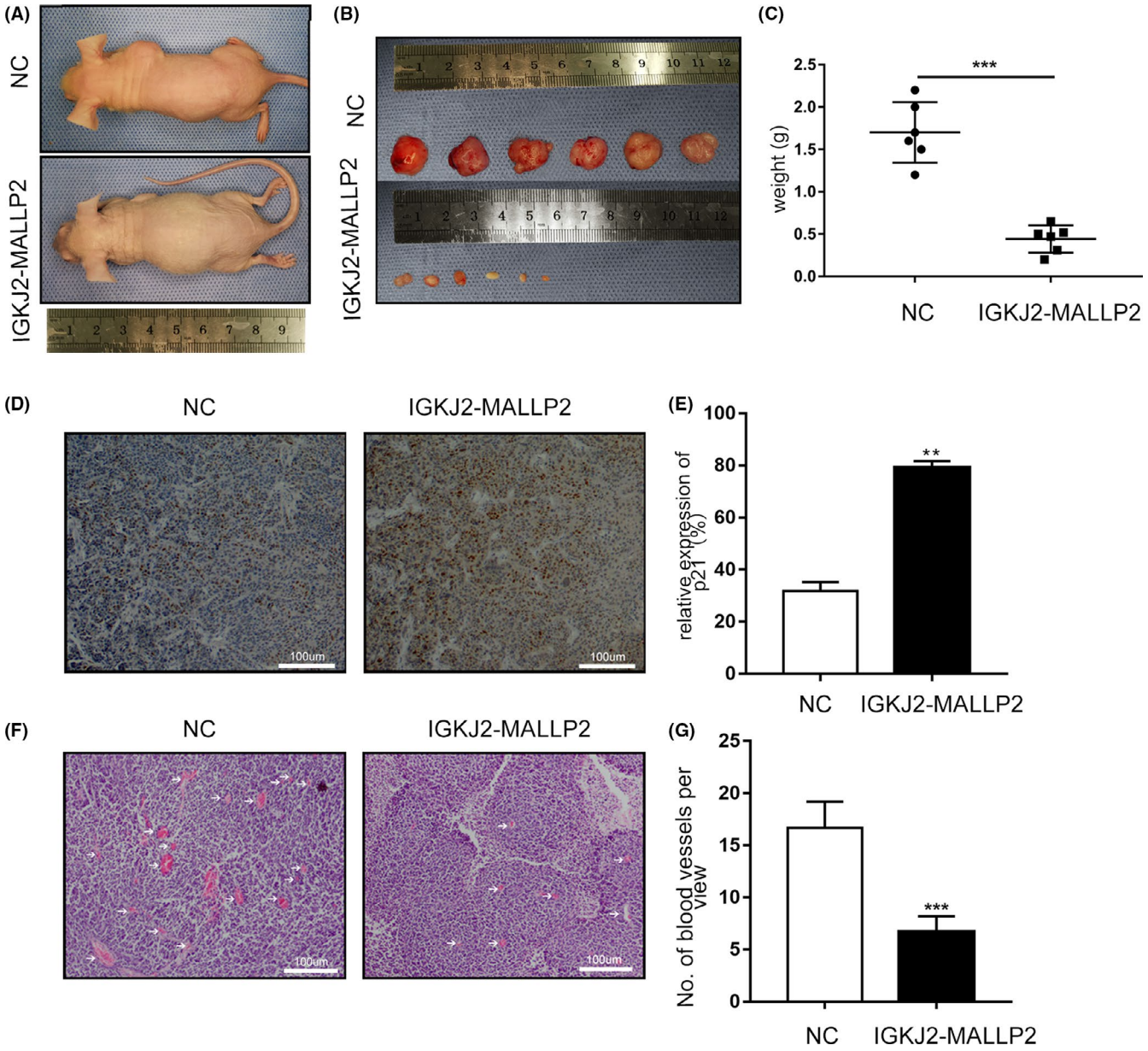

FIGURE 7 Effects of lncRNA *IGKJ2-MALLP2* on tumor growth in vivo. A, B, Representative images of xenograft tumors formed by TU212 cells transfected with NC or *IGKJ2-MALLP2* lentivirus. C, Tumor weights from NC and *IGKJ2-MALLP2* groups. D, IHC staining showed the differences in *p21* expression between the NC and *IGKJ2-MALLP2* groups, with the associated bar chart (E). F, H&E staining showing the different number of blood vessel in the 2 groups, with the associated bar chart (G). The data are presented as the means ± SD of 6 independent experiments. **, $P < .01$; ***, $P < .001$

carcinoma cells with an *IGKJ2-MALLP2* lentivirus, it inhibited the proliferation, colony formation, migration and invasion of these cells.

To determine how *IGKJ2-MALLP2* functions, the level of *IGKJ2-MALLP2* expression in the cytoplasm and nucleus of cells was assessed. The results of the present study showed that *IGKJ2-MALLP2* was primarily localized in the cytoplasm. Over recent years, studies have shown that ceRNAs represent an extremely important post-transcriptional regulatory system in which lncRNAs sponge miRNAs and sometimes degrade the targeted miRNA,[32] to alter the expression of corresponding transcribed genes thereby affecting the occurrence and development of tumors.[33] For instance, lncRNA *JPX* can upregulate *Twist1* expression via competitive sponging of *miR-33a-5p* and downregulating the expression of miR-33a-5p, and participate in the progression and lung metastasis of endometrial carcinoma through the activation of Wnt/β-catenin signaling.[34] lncRNA *Gm10451* can regulate the expression of *pTIP* mRNA by binding *miR-338-3p*, which facilitates the differentiation of Nkx6.1^{+} pancreatic progenitor cells and increases the differentiation efficiency and cell function of mature β-like cells.[35] There are also other lncRNAs that can participate in ceRNA networks and play roles in the development of carcinoma.[36] The results of the present study showed that the interaction of lncRNA *IGKJ2-MALLP2*, miRNA-*1911-3p* and *p21* formed a ceRNA network regulating laryngeal carcinoma growth and metastasis. However, further studies are required to ascertain the abundance of these 3 components and to verify the functional activity of the ceRNA.

Persistent angiogenesis plays an essential role in tumor growth and metastasis. Therefore, identifying promising anti-angiogenesis targets is considered to be an approach to treat cancer. Previous studies have reported that in colorectal cancer, the novel primate-specific lncRNA *FLANC* not only affects tumor growth but also participates in angiogenesis by regulating the STAT3/VEGF-A axis.[37] In breast cancer lncRNA *RAB11B-AS1* was reported to be induced under hypoxia and facilitate the expression of angiogenic factors (eg, VEGF-A and ANGPTL4) in breast cancer cells by facilitating recruitment of RNA polymerase II, leading to angiogenesis and metastasis in breast cancer.[38] Furthermore, regarding the relationship between *p21* and vascular endothelial growth factor A (VEGF-A), it was observed that when *p21* levels increased, VEGF-A expression decreased.[39] The identical phenomenon was also confirmed in this study. When *p21* expression was upregulated by the overexpression of *IGKJ2-MALLP2*, VEGF-A expression was downregulated, and angiogenic activities were also reduced. Furthermore, in the xenograft tumor model, we also observed that with the increased expression of *p21*, the number of blood vessels decreased. The aforementioned results indicate that low *IGKJ2-MALLP2* expression could facilitate angiogenesis by regulating *p21* expression via the mediator VEGF-A. Based on these results, we demonstrate that *IGKJ2-MALLP2* can not only regulate the function of TU212 laryngeal carcinoma cells but also the associated angiogenesis in the surrounding area.

In summary, the results of our study show that lncRNA *IGKJ2-MALLP2* can regulate *p21* expression as a ceRNA by sponging *miR-1911-3p*. *IGKJ2-MALLP2* regulates LSCC cell proliferation, colony formation, migration, and invasion. Moreover, it can also regulate angiogenesis in the area surrounding laryngeal carcinoma. A better understanding of the *IGKJ2-MALLP2/miR-1911-3p/p21* axis may provide new strategies and targets for the further treatment of laryngeal carcinoma.

ACKNOWLEDGMENTS

This study was financed by grants from the National Natural Science Foundation of China, (81572647), the Natural Science Foundation of Heilongjiang Province (LH 2019H014) and the Postgraduate Research & Practice Innovation Program of Harbin Medical University (YJSKYCX2018-48HYD).

DISCLOSURE

The authors have no conflicts of interest.

ETHICAL CONSIDERATIONS

The present study was approved by the Ethics Committee of The Second Affiliated Hospital of Harbin Medical University. The research has been carried out in accordance with the World Medical Association Declaration of Helsinki. All patients and healthy volunteers provided written informed consent prior to their inclusion within the study. All animal procedures were performed following approval from the Animal Care and Use Committee of The Second Affiliated Hospital of Harbin Medical University.

ORCID

Ming Liu https://orcid.org/0000-0002-9693-2990

REFERENCES

1. Steuer CE, El-Deiry M, Parks JR, et al. An update on larynx cancer. *CA Cancer J Clin*. 2017;67:31–50.
2. Siegel RL, Miller KD, Jemal A. Cancer statistics, 2019. *CA Cancer J Clin*. 2019;69:7–34.
3. Groome PA, O'Sullivan B, Irish JC, et al. Management and outcome differences in supraglottic cancer between Ontario, Canada, and the surveillance, epidemiology, and end results areas of the United States. *J Clin Oncol*. 2003;21:496–505.
4. Siegel RL, Miller KD, Jemal A. Cancer statistics, 2016. *CA Cancer J Clin*. 2016;66:7–30.
5. Derrien T, Johnson R, Bussotti G, et al. The GENCODE v7 catalog of human long noncoding RNAs: analysis of their gene structure, evolution, and expression. *Genome Res*. 2012;22:1775–1789.
6. Iyer MK, Niknafs YS, Malik R, et al. The landscape of long noncoding RNAs in the human transcriptome. *Nat Genet*. 2015;47:199–208.
7. Qu Z, Li S. Long noncoding RNA LINC01278 favors the progression of osteosarcoma via modulating miR-133a-3p/PTHR1 signaling. *J Cell Physiol*. 2020; https://doi.org/10.1002/jcp.29582
8. Xie Y, Dang W, Zhang S, et al. The role of exosomal noncoding RNAs in cancer. *Mol Cancer*. 2019;18:37.
9. Li H, Wang Y. Long noncoding RNA (lncRNA) MIR22HG suppresses gastric cancer progression through attenuating NOTCH2 signaling. *Med Sci Monit*. 2019;25:656–665.
10. Huang L, Wang Y, Chen J, et al. Long noncoding RNA PCAT1, a novel serum-based biomarker, enhances cell growth by sponging miR-326 in oesophageal squamous cell carcinoma. *Cell Death Dis*. 2019;10:513.

11. Seo SB, Baek JY, Lim JH, et al. 14–3-3zeta targeting induced senescence in Hep-2 laryngeal cancer cell through deneddylation of Cullin1 in the Skp1-Cullin-F-box protein complex. *Cell Prolif*. 2019;52:e12654.
12. Meng W, Cui W, Zhao L, et al. Aberrant methylation and downregulation of ZNF667-AS1 and ZNF667 promote the malignant progression of laryngeal squamous cell carcinoma. *J Biomed Sci*. 2019;26:13.
13. Liu H, Sun Y, Tian H, et al. Characterization of long non-coding RNA and messenger RNA profiles in laryngeal cancer by weighted gene co-expression network analysis. *Aging (Albany NY)*. 2019;11:10074–10099.
14. Sun S, Gong C, Yuan K. LncRNA UCA1 promotes cell proliferation, invasion and migration of laryngeal squamous cell carcinoma cells by activating Wnt/beta-catenin signaling pathway. *Exp Ther Med*. 2019;17:1182–1189.
15. Yue B, Li H, Liu M, et al. Characterization of lncRNA-miRNA-mRNA network to reveal potential functional ceRNAs in bovine skeletal muscle. *Front Genet*. 2019;10:91.
16. Zhao X, Li J, Lian B, et al. Global identification of Arabidopsis lncRNAs reveals the regulation of MAF4 by a natural antisense RNA. *Nat Commun*. 2018;9:5056.
17. Zhao R, Li FQ, Tian LL, et al. Comprehensive analysis of the whole coding and non-coding RNA transcriptome expression profiles and construction of the circRNA-lncRNA co-regulated ceRNA network in laryngeal squamous cell carcinoma. *Funct Integr Genomics*. 2019;19:109–121.
18. Bu D, Luo H, Jiao F, et al. Evolutionary annotation of conserved long non-coding RNAs in major mammalian species. *Sci China Life Sci*. 2015;58:787–798.
19. Huang Y, Li Z, Zhong Q, et al. Association of TBX2 and *P21* expression with clinicopathological features and survival of laryngeal squamous cell carcinoma. *Int J Clin Exp Med*. 2014;7:5394–5402.
20. Schmitt AM, Chang HY. Long noncoding RNAs in cancer pathways. *Cancer Cell*. 2016;29:452–463.
21. Kopp F, Mendell JT. Functional classification and experimental dissection of long noncoding RNAs. *Cell*. 2018;172:393–407.
22. Wu F, Mo Q, Wan X, et al. NEAT1/hsa-mir-98-5p/MAPK6 axis is involved in non-small-cell lung cancer development. *J Cell Biochem*. 2019;120:2836–2846.
23. Jiang P, Xu H, Xu C, et al. NEAT1 contributes to the CSC-like traits of A549/CDDP cells via activating Wnt signaling pathway. *Chem Biol Interact*. 2018;296:154–161.
24. Li S, Yang J, Xia Y, et al. Long noncoding RNA NEAT1 promotes proliferation and invasion via targeting miR-181a-5p in non-small cell lung cancer. *Oncol Res*. 2018;26:289–296.
25. Lu Y, Li T, Wei G, et al. The long non-coding RNA NEAT1 regulates epithelial to mesenchymal transition and radioresistance in through miR-204/ZEB1 axis in nasopharyngeal carcinoma. *Tumour Biol*. 2016;37:11733–11741.
26. Wang P, Wu T, Zhou H, et al. Long noncoding RNA NEAT1 promotes laryngeal squamous cell cancer through regulating miR-107/CDK6 pathway. *J Exp Clin Cancer Res*. 2016;35:22.
27. Li DY, Busch A, Jin H, et al. H19 induces abdominal aortic aneurysm development and progression. *Circulation*. 2018;138:1551–1568.
28. Merryman WD, Clark CR. Lnc-ing NOTCH1 to idiopathic calcific aortic valve disease. *Circulation*. 2016;134:1863–1865.
29. Kim J, Piao HL, Kim BJ, et al. Long noncoding RNA MALAT1 suppresses breast cancer metastasis. *Nat Genet*. 2018;50:1705–1715.
30. Gupta RA, Shah N, Wang KC, et al. Long non-coding RNA HOTAIR reprograms chromatin state to promote cancer metastasis. *Nature*. 2010;464:1071–1076.
31. Li R, Chen S, Zhan J, et al. Long noncoding RNA FOXD2-AS1 enhances chemotherapeutic resistance of laryngeal squamous cell carcinoma via STAT3 activation. *Cell Death Dis*. 2020;11:41.
32. Salmena L, Poliseno L, Tay Y, et al. A ceRNA hypothesis: the Rosetta Stone of a hidden RNA language? *Cell*. 2011;146:353–358.
33. Karreth FA, Pandolfi PP. ceRNA cross-talk in cancer: when ce-bling rivalries go awry. *Cancer Discov*. 2013;3:1113–1121.
34. Pan J, Fang S, Tian H, et al. lncRNA JPX/miR-33a-5p/Twist1 axis regulates tumorigenesis and metastasis of lung cancer by activating Wnt/beta-catenin signaling. *Mol Cancer*. 2020;19:9.
35. Huang Y, Xu Y, Lu Y, et al. lncRNA Gm10451 regulates PTIP to facilitate iPSCs-derived beta-like cell differentiation by targeting miR-338-3p as a ceRNA. *Biomaterials*. 2019;216:119266.
36. Li Z, Cai B, Abdalla BA, et al. LncIRS1 controls muscle atrophy via sponging miR-15 family to activate IGF1-PI3K/AKT pathway. *J Cachexia Sarcopenia Muscle*. 2019;10:391–410.
37. Pichler M, Rodriguez-Aguayo C, Nam SY, et al. Therapeutic potential of FLANC, a novel primate-specific long non-coding RNA in colorectal cancer. *Gut*. 2020. https://doi.org/10.1136/gutjnl-2019-318903
38. Niu Y, Bao L, Chen Y, et al. HIF-2-induced long non-coding RNA RAB11B-AS1 promotes hypoxia-mediated angiogenesis and breast cancer metastasis. *Cancer Res*. 2020;80:964–975.
39. Luo H, Rankin GO, Juliano N, et al. Kaempferol inhibits VEGF expression and in vitro angiogenesis through a novel ERK-NFkappaB-cMyc-*p21* pathway. *Food Chem*. 2012;130:321–328.

How to cite this article: Cao J, Yang Z, An R, et al. lncRNA *IGKJ2-MALLP2* suppresses LSCC proliferation, migration, invasion, and angiogenesis by sponging *miR-1911-3p/p21*. *Cancer Sci*. 2020;111:3245–3257. https://doi.org/10.1111/cas.14559